Res Chem Intermed (2018) 44:5013–5029
https://doi.org/10.1007/s11164-018-3406-0

Synthesis of 3,4,5-substituted furan-2(5*H*)-ones using Al-doped ZnO nanostructure

Majid Ghashang[1] · Sadaf Janghorban[1] · Seyyed Jalal Roudbaraki[2]

Received: 24 November 2017 / Accepted: 19 March 2018 / Published online: 26 March 2018

Abstract Al-doped ZnO nanostructures were prepared via a simple precipitation method and were characterized by several techniques including XRD, TEM, EDX, UV–Vis, and DLS. All XRD patterns show the hexagonal single-phase structure of pure and Al-doped ZnO nanopowders without impurity. The samples consist of particles with average sizes ranging from 53 to 60 nm measured by DLS technique. Next, the catalytic activity of pure and Al-doped ZnO nanopowders was investigated in terms of synthesis of 3,4,5-substituted furan-2(5*H*)-one derivatives using the three-component reaction of aldehydes, aromatic amines, and acetylenic esters. This procedure has advantages such as high yields, simple methodology, and easy work-up.

Keywords 3,4,5-substituted furan-2(5*H*)-one · Al-doped ZnO · ZnO · Acetylenic esters · Butenolides

Introduction

Furan-2(5*H*)-ones are a class of butenolides of major interest not only for their presence in several biologically active compounds but also for their use as synthetic intermediates [1–7]. In recent years, butenolide derivatives have been exploited successfully as antimicrobial [8, 9], antifungal [10, 11], anti-inflammatory [12], anticancer [13, 14] and anti-viral HIV-1 agents [15, 16]. Due to the high

✉ Majid Ghashang
ghashangmajid@gmail.com

[1] Department of Chemistry, Faculty of Sciences, Najafabad Branch, Islamic Azad University, P.O. Box 517, Najafabad, Iran

[2] Department of Chemistry, Faculty of Sciences, Lahijan Branch, Islamic Azad University, Lahijan, Iran

significance of substituted furan-2(5*H*)-ones in applications as effective drugs, it is important to synthesize these compounds via a simple and efficient method. To date, diverse synthetic methods have been reported including Passerini-like three-component condensation [17], exo-selective cycloisomerization of acetylenic acids [18], gold-catalyzed condensation reaction of alkynes, amines, and glyoxylic acid [19], cross-coupling of allenyl carboxylic acids with vinyl/aryl halides catalyzed by Pd–Ag [20], *N*-heterocyclic carbene catalyzed transformations [21], C–H activation reaction of cyclo-alkenecarboxylic acids and acrylates [22], Morita–Baylis–Hillman adducts [23], and three-component reaction of amines, aldehydes, and acetylenic esters [24]. The latter method was designed for the synthesis of 3,4,5-substituted furan-2(5*H*)-ones and was promoted by a few Lewis and Brønsted acids including β-cyclodextrin [24], $SnCl_2$ [25], ZnO nanoparticles [26, 27], $Al(HSO_4)_3$ [28], tetra-*n*-butylammonium bisulfate [29], PPA/SiO_2 [30], SnO nanoparticles [31], and HY zeolite [32].

The widespread interest in the chemistry and therapeutic application of furan-2(5*H*)-one derivatives stimulate us to continue our works on multi-component reactions [33–44] and develop a new method for the preparation of 3,4,5-substituted furan-2(5*H*)-ones using a novel nanostructure of Al-doped ZnO as a stable heterogeneous catalyst (Scheme 1).

Experimental

Reagents and instrumentation

Chemicals were purchased from Merck and Aldrich and used without further purification. The catalyst characterizations were conducted on a HITACHI S-4160 field emission scanning electron microscope (FE-SEM) and a Bruker-AXS Advance D8 X-ray diffractometer with Cu-Kα irradiation. The nuclear magnetic resonance (NMR) spectra were recorded on a Bruker Avance DPX 400 MHz instrument. The spectra were measured in DMSO-d_6 relative to TMS (0.00 ppm). Elemental analysis was performed on a Heraeus CHN-O-Rapid analyzer. Thin-layer chromatography (TLC) was performed on silica gel Polygram SIL G/UV 254 plates.

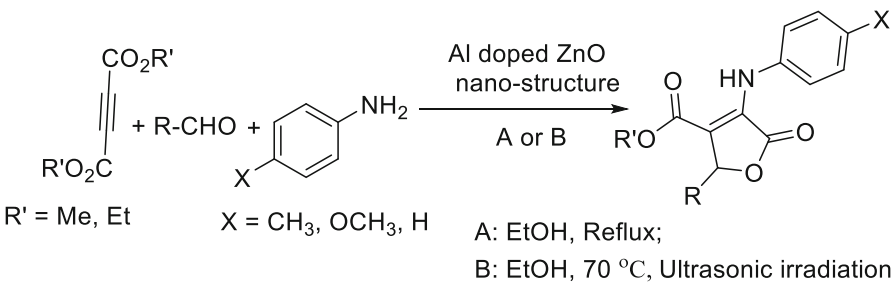

Scheme 1 Preparation of 3,4,5-substituted furan-2(5*H*)-one derivatives

Preparation of nanostructured Al-doped ZnO

An aqueous ammonia solution (37%) was diluted by water (30 mL) and was drop-wise added into a solution of mixed $Al(NO_3)_3$ (1 mmol) and $Zn(NO_3)_2$ (20 mmol) in 50 mL of distilled water drop-wise under magnetic stirring. The obtained mixture was stirred at room temperature for 30 min. The precipitate was filtered, washed with distilled water, and dried. The precipitate was calcined at 500 °C in an electric furnace for 2 h.

General procedure

Aldehyde (1 mmol), acetylenic esters (1 mmol), aromatic amine (1 mmol), nanostructured Al-doped ZnO (0.025 g), and ethanol (5 mL) was charged into a round-bottom flask. The resulting mixture was stirred at reflux condition for the appropriate time (Table 4, monitored by TLC). Upon completion, the solvent was concentrated and the reaction mixture was diluted in $CHCl_3$; simple filtration isolated the catalyst and the crude product was washed with diethyl ether to afford the pure product.

Selected data:

Methyl 2-(benzofuran-2-yl)-5-oxo-4-(phenylamino)-2,5-dihydrofuran-3-carboxylate (**18a**): ^{1}H-NMR (400 MHz, DMSO-d_6): 3.75 (s, 3H, OCH_3), 6.37 (s, 1H), 6.88 (s, 1H), 7.09 (t, J = 7.6 Hz, 1H), 7.25–7.31 (m, 2H), 7.48–7.60 (m, 6H), 9.97 (s, 1H, NH) ppm; ^{13}C-NMR (100 MHz, DMSO-d_6): 52.3, 69.6, 105.8, 112.0, 121.2, 121.9, 123.6, 124.8, 126.0, 126.8, 129.3, 129.4, 131.3, 140.8, 155.2, 157.1, 163.2, 166.1 ppm; found: C, 68.90; H, 4.49; N, 4.17 $C_{20}H_{15}NO_5$; requires: C, 68.76; H, 4.33; N, 4.01%.

Ethyl 2-(benzofuran-2-yl)-5-oxo-4-(phenylamino)-2,5-dihydrofuran-3-carboxylate (**19a**): ^{1}H-NMR (400 MHz, DMSO-d_6): 1.27 (t, J = 6.8 Hz, 3H, CH_3), 4.16 (q, J = 6.8 Hz, 2H, OCH_2), 6.38 (s, 1H), 6.93 (s, 1H), 7.08 (t, J = 7.6 Hz, 1H), 7.25–7.31 (m, 2H), 7.47–7.61 (m, 6H), 10.02 (s, 1H, NH) ppm; ^{13}C-NMR (100 MHz, DMSO-d_6): 14.2, 61.0, 69.8, 105.9, 111.9, 121.1, 121.8, 123.4, 124.8, 126.0, 126.8, 129.3, 129.4, 131.2, 140.8, 155.1, 157.0, 163.5, 166.3 ppm; found: C, 69.52; H, 4.87; N, 4.01 $C_{21}H_{17}NO_5$; requires: C, 69.41; H, 4.72; N, 3.85%.

Methyl 2-(benzofuran-2-yl)-5-oxo-4-(*p*-tolylamino)-2,5-dihydrofuran-3-carboxylate (**20a**): ^{1}H-NMR (400 MHz, DMSO-d_6): 2.22 (s, 3H, CH_3), 3.75 (s, 3H, OCH_3), 6.36 (s, 1H), 6.89 (s, 1H), 7.07–7.17 (m, 4H), 7.26–7.32 (m, 2H), 7.52–7.56 (m, 2H), 10.04 (s, 1H, NH) ppm; ^{13}C-NMR (100 MHz, DMSO-d_6): 21.5, 52.1, 70.0, 105.9, 111.9, 113.0, 121.8, 123.6, 125.8, 126.8, 129.3, 129.6, 131.2, 132.7, 141.0, 155.1, 157.1, 163.2, 166.1 ppm; found: C, 69.55; H, 4.89; N, 3.97 $C_{21}H_{17}NO_5$; requires: C, 69.41; H, 4.72; N, 3.85%.

Ethyl 2-(benzofuran-2-yl)-5-oxo-4-(*p*-tolylamino)-2,5-dihydrofuran-3-carboxylate (**21a**): ^{1}H-NMR (400 MHz, DMSO-d_6): 1.25 (t, J = 6.8 Hz, 3H, CH_3), 2.23 (s, 3H, CH_3), 4.16 (q, J = 6.8 Hz, 2H, OCH_2), 6.34 (s, 1H), 6.91 (s, 1H), 7.09–7.16 (m, 4H), 7.27–7.31 (m, 2H), 7.52–7.56 (m, 2H), 10.08 (s, 1H, NH) ppm; ^{13}C-NMR (100 MHz, DMSO-d_6): 14.2, 21.5, 60.8, 69.9, 106.0, 111.8, 113.0, 121.9, 123.4,

125.8, 126.9, 129.4, 129.7, 131.3, 132.5, 140.8, 155.3, 157.2, 163.1, 166.2 ppm; found: C, 70.21; H, 5.23; N, 3.80 $C_{22}H_{19}NO_5$; requires: C, 70.02; H, 5.07; N, 3.71%.

Methyl 2-(benzofuran-2-yl)-4-((3,4-dimethylphenyl)amino)-5-oxo-2,5-dihydrofuran-3-carboxylate (**22a**): ^{1}H-NMR (400 MHz, DMSO-d_6): 2.21 (s, 3H, CH_3), 2.25 (s, 3H, CH_3), 3.75 (s, 3H, OCH_3), 6.48 (s, 1H), 6.69 (d, J = 8.0 Hz, 1H), 6.80–6.87 (m, 2H), 7.25–7.31 (m, 2H), 7.41 (s, 1H), 7.51–7.56 (m, 2H), 10.14 (s, 1H, NH) ppm; ^{13}C-NMR (100 MHz, DMSO-d_6): 19.8, 20.7, 52.3, 73.2, 107.6, 112.1, 117.3, 120.8, 121.9, 124.1, 126.1, 127.0, 129.4, 130.3, 131.5, 132.4, 136.1, 141.1, 154.7, 157.2, 162.1, 165.1 ppm; found: C, 70.21; H, 5.24; N, 3.85 $C_{22}H_{19}NO_5$; requires: C, 70.02; H, 5.07; N, 3.71%.

Ethyl 2-(benzofuran-2-yl)-4-((3,4-dimethylphenyl)amino)-5-oxo-2,5-dihydrofuran-3-carboxylate (**23a**): ^{1}H-NMR (400 MHz, DMSO-d_6): 1.27 (t, J = 6.8 Hz, 3H, OCH_2CH_3), 2.20 (s, 3H, CH_3), 2.24 (s, 3H, CH_3), 4.16 (q, J = 6.8 Hz, 2H, OCH_2), 6.47 (s, 1H), 6.71 (d, J = 8.0 Hz, 1H), 6.81–6.88 (m, 2H), 7.24–7.31 (m, 2H), 7.40 (s, 1H), 7.51–7.56 (m, 2H), 10.11 (s, 1H, NH) ppm; ^{13}C-NMR (100 MHz, DMSO-d_6): 14.3, 19.9, 21.0, 61.2, 73.4, 107.8, 112.2, 117.5, 120.7, 121.8, 124.0, 126.2, 127.0, 129.3, 130.4, 131.6, 132.5, 136.0, 141.0, 154.6, 157.0, 162.2, 165.1 ppm; found: C, 70.86; H, 5.69; N, 3.77 $C_{23}H_{21}NO_5$; requires: C, 70.58; H, 5.41; N, 3.58%.

Methyl 4-((3,4-dimethylphenyl)amino)-5-oxo-2-phenyl-2,5-dihydrofuran-3-carboxylate (**24a**): ^{1}H-NMR (400 MHz, DMSO-d_6): 2.21 (s, 3H, CH_3), 2.25 (s, 3H, CH_3), 3.74 (s, 3H, OCH_3), 6.06 (s, 1H), 6.69 (d, J = 7.9 Hz, 1H), 6.89 (d, J = 7.9 Hz, 1H), 7.31–7.39 (m, 4H), 7.45 (d, J = 7.8 Hz, 2H), 9.25 (s, 1H, NH) ppm; ^{13}C-NMR (100 MHz, DMSO-d_6): 19.8, 21.1, 52.3, 86.6, 117.2, 121.1, 128.6, 128.9, 129.3, 129.7, 130.4, 131.4, 132.7, 135.1, 136.0, 141.2, 162.3, 164.9 ppm; found: C, 71.45; H, 5.91; N, 4.31 $C_{20}H_{19}NO_4$; requires: C, 71.20; H, 5.68; N, 4.15%.

Ethyl 4-((3,4-dimethylphenyl)amino)-5-oxo-2-phenyl-2,5-dihydrofuran-3-carboxylate (**25a**): ^{1}H-NMR (400 MHz, DMSO-d_6): 1.27 (t, J = 6.8 Hz, 3H, OCH_2CH_3), 2.21 (s, 3H, CH_3), 2.25 (s, 3H, CH_3), 4.15 (q, J = 6.8 Hz, 2H, OCH_2), 6.07 (s, 1H), 6.68 (d, J = 7.9 Hz, 1H), 6.88 (d, J = 7.9 Hz, 1H), 7.29–7.40 (m, 6H), 9.08 (s, 1H, NH) ppm; ^{13}C-NMR (100 MHz, DMSO-d_6): 14.4, 19.9, 21.1, 61.2, 86.7, 117.3, 121.2, 128.5, 128.9, 129.3, 129.6, 123.4, 131.4, 132.6, 135.0, 136.1, 141.1, 162.2, 165.1 ppm; found: C, 71.93; H, 6.22; N, 4.11 $C_{21}H_{21}NO_4$; requires: C, 71.78; H, 6.02; N, 3.99%.

Methyl 4-((3,4-dimethylphenyl)amino)-5-oxo-2-(*p*-tolyl)-2,5-dihydrofuran-3-carboxylate (**26a**): ^{1}H-NMR (400 MHz, DMSO-d_6): 2.20 (s, 3H, CH_3), 2.24 (s, 3H, CH_3), 2.28 (s, 3H, CH_3), 3.75 (s, 3H, OCH_3), 6.25 (s, 1H), 6.69 (d, J = 8.0 Hz, 1H), 6.89 (d, J = 8.0 Hz, 1H), 7.14–7.20 (m, 4H), 7.41 (s, 1H), 8.98 (s, 1H, NH) ppm; ^{13}C-NMR (100 MHz, DMSO-d_6): 19.8, 21.0, 21.6, 52.3, 86.8, 117.4, 121.2, 126.6, 129.3, 129.6, 130.2, 131.5, 132.7, 135.2, 136.3, 140.1, 141.1, 162.4, 165.1 ppm; found: C, 71.97; H, 6.23; N, 4.17 $C_{21}H_{21}NO_4$; requires: C, 71.78; H, 6.02; N, 3.99%.

Ethyl 4-((3,4-dimethylphenyl)amino)-5-oxo-2-(*p*-tolyl)-2,5-dihydrofuran-3-carboxylate (**27a**): ^{1}H-NMR (400 MHz, DMSO-d_6): 1.26 (t, J = 6.8 Hz, 3H, OCH_2CH_3), 2.20 (s, 3H, CH_3), 2.24 (s, 3H, CH_3), 2.27 (s, 3H, CH_3), 4.17 (q, J = 6.8 Hz, 2H, OCH_2), 6.27 (s, 1H), 6.68 (d, J = 7.9 Hz, 1H), 6.90 (d, J = 7.9 Hz, 1H),

7.14–7.21 (m, 4H), 7.41 (s, 1H), 9.03 (s, 1H, NH) ppm; ^{13}C-NMR (100 MHz, DMSO-d_6): 14.5, 19.9, 21.2, 21.6, 61.1, 86.9, 117.4, 121.2, 126.7, 129.3, 129.7, 130.2, 131.5, 132.6, 135.4, 136.6, 140.2, 141.3, 162.4, 165.2 ppm; found: C, 72.55; H, 6.59; N, 4.00 $C_{22}H_{23}NO_4$; requires: C, 72.31; H, 6.34; N, 3.83%.

Methyl 2-(4-chlorophenyl)-4-((3,4-dimethylphenyl)amino)-5-oxo-2,5-dihydrofuran-3-carboxylate (**28a**): ^{1}H-NMR (400 MHz, DMSO-d_6): 2.22 (s, 3H, CH_3), 2.26 (s, 3H, CH_3), 3.75 (s, 3H, OCH_3), 6.21 (s, 1H), 6.70 (d, J = 8.0 Hz, 1H), 6.90 (d, J = 8.0 Hz, 1H), 7.40 (s, 1H), 7.46 (d, J = 7.9 Hz, 2H), 7.58 (d, J = 7.9 Hz, 2H), 9.34 (s, 1H, NH) ppm; ^{13}C-NMR (100 MHz, DMSO-d_6): 19.9, 21.1, 52.4, 87.0, 117.4, 121.3, 127.8, 129.0, 129.5, 130.4, 131.3, 132.7, 135.2, 136.8, 136.9, 141.2, 162.4, 165.3 ppm; found: C, 64.84; H, 5.06; N, 3.91 $C_{20}H_{18}ClNO_4$; requires: C, 64.61; H, 4.88; N, 3.77%.

Methyl 2-(3-chlorophenyl)-4-((3,4-dimethylphenyl)amino)-5-oxo-2,5-dihydrofuran-3-carboxylate (**29a**): ^{1}H-NMR (400 MHz, DMSO-d_6): 2.21 (s, 3H, CH_3), 2.25 (s, 3H, CH_3), 3.74 (s, 3H, OCH_3), 6.17 (s, 1H), 6.70 (d, J = 7.8 Hz, 1H), 6.90 (d, J = 7.8 Hz, 1H), 7.19–7.28 (m, 2H), 7.40–7.43 (m, 2H), 7.54 (s, 1H), 9.19 (s, 1H, NH) ppm; ^{13}C-NMR (100 MHz, DMSO-d_6): 19.9, 21.2, 52.5, 86.9, 117.3, 121.4, 126.7, 127.7, 129.6, 129.9, 130.4, 130.6, 132.2, 132.7, 132.9, 136.7, 137.6, 141.2, 162.1, 165.2 ppm; found: C, 64.91; H, 5.12; N, 3.97 $C_{20}H_{18}ClNO_4$; requires: C, 64.61; H, 4.88; N, 3.77%.

Methyl 2-(2-chlorophenyl)-4-((3,4-dimethylphenyl)amino)-5-oxo-2,5-dihydrofuran-3-carboxylate (**30a**): ^{1}H-NMR (400 MHz, DMSO-d_6): 2.21 (s, 3H, CH_3), 2.25 (s, 3H, CH_3), 3.74 (s, 3H, OCH_3), 6.22 (s, 1H), 6.69 (d, J = 7.9 Hz, 1H), 6.89 (d, J = 7.9 Hz, 1H), 7.26–7.31 (m, 2H), 7.39 (s, 1H), 7.53–7.59 (m, 2H), 9.07 (s, 1H, NH) ppm; ^{13}C-NMR (100 MHz, DMSO-d_6): 19.8, 21.2, 52.3, 87.0, 117.4, 121.2, 127.6, 129.3, 129.8, 130.2, 130.5, 130.7, 131.7, 132.6, 133.0, 136.7, 137.3, 141.2, 162.3, 165.2 ppm; found: C, 64.89; H, 5.11; N, 3.93 $C_{20}H_{18}ClNO_4$; requires: C, 64.61; H, 4.88; N, 3.77%.

Methyl 2-(4-(tert-butyl)phenyl)-4-((3,4-dimethylphenyl)amino)-5-oxo-2,5-dihydrofuran-3-carboxylate (**31a**): ^{1}H-NMR (400 MHz, DMSO-d_6): 1.27 (s, 9H), 2.20 (s, 3H, CH_3), 2.24 (s, 3H, CH_3), 3.75 (s, 3H, OCH_3), 6.27 (s, 1H), 6.69 (d, J = 8.0 Hz, 1H), 6.89 (d, J = 8.0 Hz, 1H), 7.08 (d, J = 7.9 Hz, 2H), 7.23 (d, J = 7.9 Hz, 2H), 7.39 (s, 1H), 8.87 (s, 1H, NH) ppm; ^{13}C-NMR (100 MHz, DMSO-d_6): 19.9, 21.1, 31.7, 34.9, 52.3, 86.8, 117.3, 121.2, 125.4, 126.8, 129.4, 130.2, 131.4, 132.7, 134.8, 136.3, 141.1, 153.7, 162.3, 165.1 ppm; found: C, 73.43; H, 7.11; N, 3.74 $C_{24}H_{27}NO_4$; requires: C, 73.26; H, 6.92; N, 3.56%.

Methyl 4-((3,4-dimethylphenyl)amino)-2-(4-methoxyphenyl)-5-oxo-2,5-dihydrofuran-3-carboxylate (**32a**): ^{1}H-NMR (400 MHz, DMSO-d_6): 2.20 (s, 3H, CH_3), 2.24 (s, 3H, CH_3), 3.74 (s, 3H, OCH_3), 3.76 (s, 3H, OCH_3), 6.39 (s, 1H), 6.69 (d, J = 7.9 Hz, 1H), 6.89 (d, J = 7.9 Hz, 1H), 6.98 (d, J = 7.9 Hz, 2H), 7.38–7.41 (m, 3H), 8.56 (s, 1H, NH) ppm; ^{13}C-NMR (100 MHz, DMSO-d_6): 19.9, 21.2, 52.3, 55.7, 86.9, 114.4, 117.3, 121.1, 125.3, 129.4, 130.2, 131.5, 132.6, 135.2, 136.4, 141.2, 160.3, 162.4, 165.3 ppm; found: C, 68.86; H, 5.99; N, 4.02 $C_{21}H_{21}NO_5$; requires: C, 68.65; H, 5.76; N, 3.81%.

Methyl 4-((3,4-dimethylphenyl)amino)-2-(3-methoxyphenyl)-5-oxo-2,5-dihydrofuran-3-carboxylate (**33a**): ^{1}H-NMR (400 MHz, DMSO-d_6): 2.20 (s, 3H, CH_3), 2.24

(s, 3H, CH_3), 3.74 (s, 3H, OCH_3), 3.75 (s, 3H, OCH_3), 6.19 (s, 1H), 6.69 (d, J = 7.8 Hz, 1H), 6.88–6.91 (m, 2H), 7.06 (s, 1H), 7.10 (d, J = 7.9 Hz, 1H), 7.29 (t, J = 7.9 Hz, 1H), 7.39 (s, 1H), 8.74 (s, 1H, NH) ppm; ^{13}C-NMR (100 MHz, DMSO-d_6): 19.8, 21.0, 52.4, 55.7, 86.8, 111.2, 115.2, 117.3, 121.1, 126.5, 129.4, 130.2, 130.5, 131.7, 132.6, 136.4, 137.7, 141.0, 159.5, 162.4, 165.0 ppm; found: C, 68.84; H, 5.96; N, 3.98 $C_{21}H_{21}NO_5$; requires: C, 68.65; H, 5.76; N, 3.81%.

Methyl 4-((3,4-dimethylphenyl)amino)-5-oxo-2-(*o*-tolyl)-2,5-dihydrofuran-3-carboxylate (**34a**): ^{1}H-NMR (400 MHz, DMSO-d_6): 2.20 (s, 3H, CH_3), 2.24 (s, 3H, CH_3), 2.25 (s, 3H, CH_3), 3.74 (s, 3H, OCH_3), 6.21 (s, 1H), 6.69 (d, J = 7.9 Hz, 1H), 6.88–6.95 (m, 2H), 7.06–7.19 (m, 4H), 7.39 (s, 1H), 8.64 (s, 1H, NH) ppm; ^{13}C-NMR (100 MHz, DMSO-d_6): 19.9, 21.1, 19.7, 52.3, 86.7, 117.3, 121.0, 126.5, 128.5, 129.4, 129.9, 130.2, 130.7, 131.6, 132.7, 135.6, 136.1, 137.2, 141.1, 162.3, 165.1 ppm; found: C, 71.94; H, 6.29; N, 4.26 $C_{21}H_{21}NO_4$; requires: C, 71.78; H, 6.02; N, 3.99%.

Result and discussion

Catalyst characterization

To obtain information about the phase characteristics of the synthesized materials, X-ray diffraction (XRD) analysis was performed. Figure 1 shows the XRD patterns of pure and Al-doped ZnO nanopowders calcined at 500 °C for 2 h. The hexagonal single-phase structure (space group P63mc) was observed in the XRD pattern of the powders which is in agreement with the reported standard values (JCPDS 01-079-

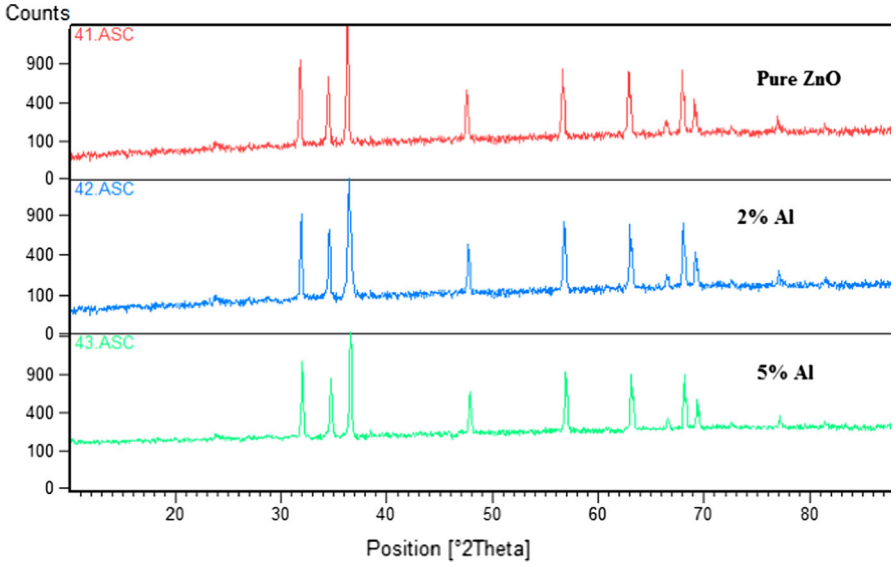

Fig. 1 XRD pattern of pure and Al-doped ZnO nanostructure

2205) [45]. The characteristic peaks of hexagonal ZnO are 31.76, 34.42, 36.25, 47.52, 56.56, 62.81, 66.40, 67.88, 69.03, and 76.90 [2θ°]. The XRD patterns do not show impurity peaks related to Al phases which indicates that Al ions were entirely substituted by Zn sites in the lattices of ZnO crystal. Also, the highest peak (36.25 2θ°) for pure ZnO led to a positive change in the broadening and location which agrees with decreasing the grain size (Fig. 2). The crystalline size, microstrain (ε), and dislocation density of the samples were determined from the full width at half maximum (FWHM) of the highest peak of the XRD pattern (Table 1). The crystal sizes of the samples are 61, 50, and 56 nm for pure ZnO, 2% Al, and 5% Al, respectively. A smaller crystal size was observed for the sample containing 2% Al, and after that, it decreased with the increase of Al concentration. In general, because of smaller crystal size, the microstrain and dislocation density of Al-doped ZnO samples are bigger than those of pure ZnO [45].

Transmission electron microscopy (TEM) analysis was used to determine the morphological structure of the nanostructured ZnO and Al-doped ZnO (Fig. 3). The particles are homogeneous and nearly uniformly spherical with dimensions less than 100 nm. The results show that the shape of the doped particles does not change obviously compared with pure ZnO. The chemical composition of pure ZnO and Al-doped ZnO nanostructures were determined by energy-dispersive X-ray spectroscopy (EDX) analysis (Fig. 4). The results of EDX analysis confirm the chemical constituents of three samples (0, 0.69, and 1.69% of Al element). The dynamic light-scattering (DLS) technique was used to determine the particle size distribution of the pure ZnO and Al-doped ZnO nanostructure samples. Before analysis, 1 g of each sample was dispersed in 20 mL of ethanol by ultrasonic irradiation for 30 min. According to DLS measurement, the nanoparticles have an average size of 60 (pure ZnO), 56 (2% Al), and 53 nm (5% Al; Fig. 5).

The UV absorption spectra of pure ZnO and Al-doped ZnO nanostructures samples show strong absorption peaks at 360, 356, and 349 nm for pure ZnO, 2%

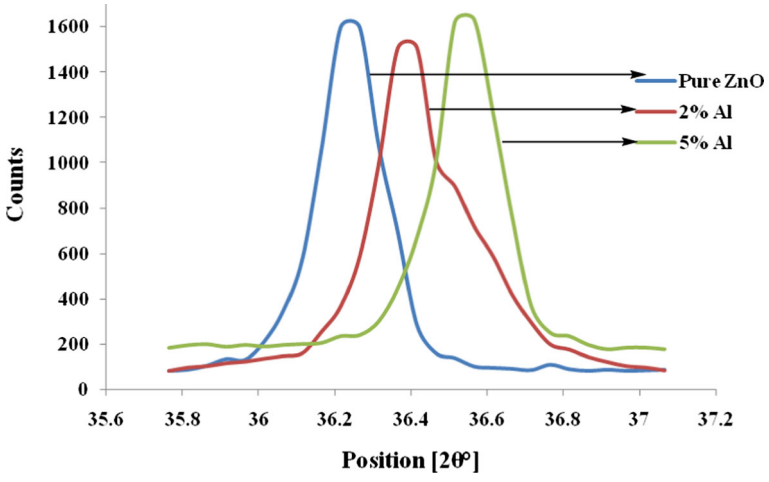

Fig. 2 Changes in the broadening and location of the highest peak (36.25 2θ°)

Table 1 Data of high-intensity XRD peaks for pure and Al-doped ZnO nanostructures

Sample	Crystal system (space group)	Peak position ($2\theta^{\circ}$)	FWHM β ($2\theta^{\circ}$)	Average crystallite size A (nm) $A = \frac{0.9\lambda}{\beta\cos\theta}$	Microstrain (ε) $\varepsilon = \frac{\beta\cos\theta}{4}$	Dislocation density (δ) $\delta = \frac{1}{A^2}$
Pure ZnO	Hexagonal (P63mc)	36.2516	0.2357	61.874	0.056	2.612×10^{-4}
2% Al	Hexagonal (P63mc)	36.4019	0.2863	50.917	0.068	3.857×10^{-4}
5% Al	Hexagonal (P63mc)	36.557	0.2569	56.818	0.061	3.098×10^{-4}

Al, and 5% Al samples, respectively (Fig. 6). From the theory of the Moss–Burstein effect, there is a blue shift with simultaneous peak broadening in the peaks related to Al-doped ZnO samples compared with pure ZnO [39]. The samples' band gaps were calculated as 3.45 (pure ZnO), 3.49 (2% Al), and 3.56 (5% Al) from the following equation:

$$E(ev) = \frac{1241}{\lambda(\mathrm{nm})}$$

where λ(nm) is the absorption peaks of the samples.

The increase in the band gap of the samples from pure ZnO to 5% Al impurity is due to the quantum size effect which causes a blue shift in the absorption [46].

Brunauer–Emmet–Teller (BET) surface area technique was used to determine the specific surface area of the samples as 30.14 $m^2\ g^{-1}$ (2% Al), 29.64 $m^2\ g^{-1}$ (5% Al), and 9.97 $m^2\ g^{-1}$ for pure ZnO.

Investigation of the catalytic activity

At first, the catalytic activities for the synthesis of **4** through the transformation of **1**, **2**, and **3** using some of the metal oxides were measured to elucidate the effect of metal oxides (Scheme 2, Table 2). The order of metal oxides on the **4** formation rate is Al-doped ZnO (2% Al) > Al-doped ZnO (5% Al) > ZnO > MgO > SnO_2. Some catalysts, including Al_2O_3, SiO_2, Fe_2O_3, and CaO, were found to be non-effective in the reaction. In this study, Al-doped ZnO was found to be a more effective catalyst for **4** (85% yield) synthesis than ZnO (80% yield) which is a suitable metal oxide for the above transformation. Doping of Al promoted the catalytic activity of ZnO (Table 2).

The results of performed experiments showed that the solvent has an anomalous effect on the productivity of the reaction (Table 3). Unlike polar solvents which have to result in moderate to good yields, use of non-polar solvents and also solvent-free condition is not effective. Consequently, per the obtained results, EtOH is the more suitable solvent for the reaction medium. Next, the effect of catalyst dosage (varying from 0.1 to 1 mmol) on the product yield was investigated. An excellent

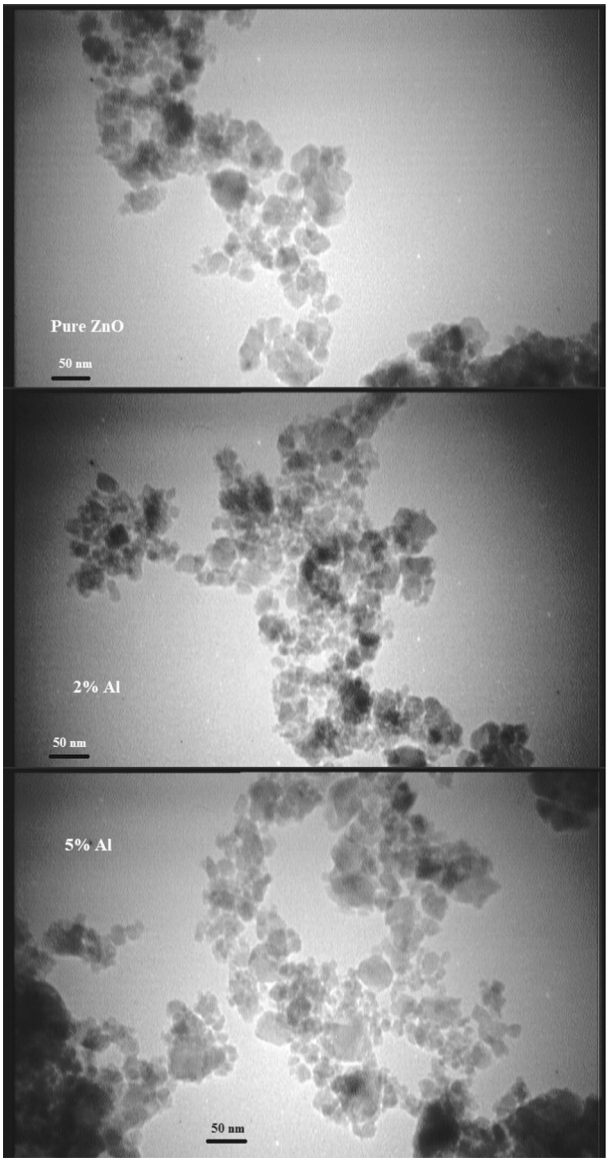

Fig. 3 TEM images of pure ZnO and Al-doped ZnO nanostructures

yield of product was obtained when 0.3 mmol of catalyst was used. The further increase in the catalyst dosage did not show any significant increase in the product yield (Table 3).

A plausible proposed mechanism for the formation of 3,4,5-substituted furan-2(5*H*)-ones is shown in Scheme 3. At first, the nucleophilic attack of an aromatic amine to dialkyl acetylenedicarboxylate results in the generation of intermediate

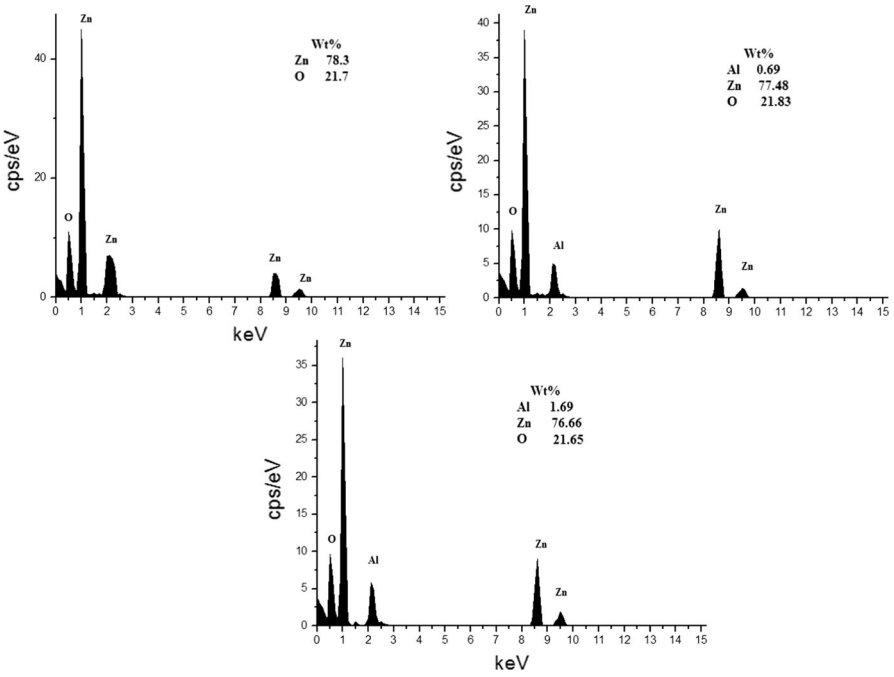

Fig. 4 Chemical composition of pure ZnO and Al-doped ZnO nanostructures using EDX analysis

a. At the same time, aromatic aldehyde was activated by Al-doped ZnO as a catalyst to form an activated carbonyl group (**b**). Subsequently, the reaction of intermediate **a** with activated aromatic aldehyde to form intermediate **c** which is equilibrated with intermediate **d**. The cyclization reaction produced 3,4,5-substituted furan-2(5*H*)-ones.

Although the rule of Al-doped ZnO in catalytic processes is the same with those of pure ZnO, the product yields for doped samples are higher which may be due to the higher surface area of doped samples (30.14 and 29.64 $m^2\ g^{-1}$) compared with pure ZnO (9.97 $m^2\ g^{-1}$).

Next, using the optimized conditions (Table 3: catalyst (0.3 mmol), ethanol, reflux), diverse anilines, aldehydes, and acetylenic esters reacted together to give the corresponding 3,4,5-substituted furan-2(5*H*)-ones (Scheme 1, Table 4). It was found that the yields and product purity for all products including electron-donating and electron-withdrawing groups (EDGs and EWGs, respectively) substituted on the aromatic rings are good (Table 4, products **1a**–**34a**). Aromatic aldehydes and amines bearing EWGs require more time to complete the reaction, whereas this time is less for the donor substitutions. The substitution groups in the *ortho* position will increase reaction time.

In contrast with the substitution of the EDG such as methyl (**3a**, **4a**) or *tert*-butyl (**6a**, **7a**), aldehydes bearing EWGs such as chlorine (**5a**) showed diminished activity. The activity of aromatic aldehydes can be increased when they are coordinated to the ZnO catalyst. The capability of the carbonyl coordination of

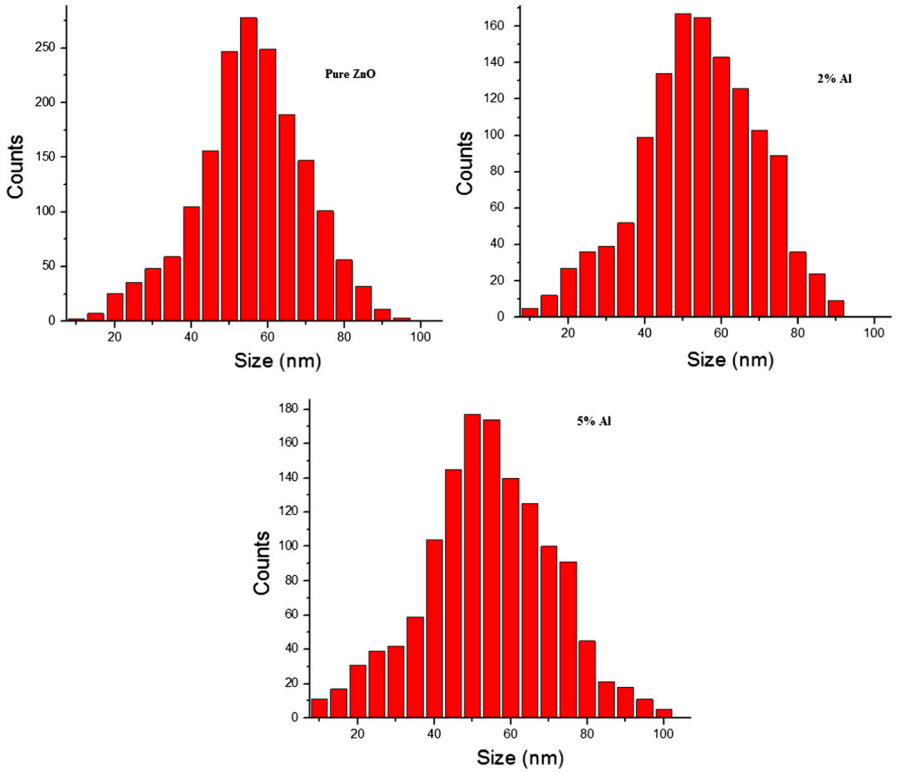

Fig. 5 Particle size distribution analysis of pure ZnO and Al-doped ZnO nanostructures using DLS technique

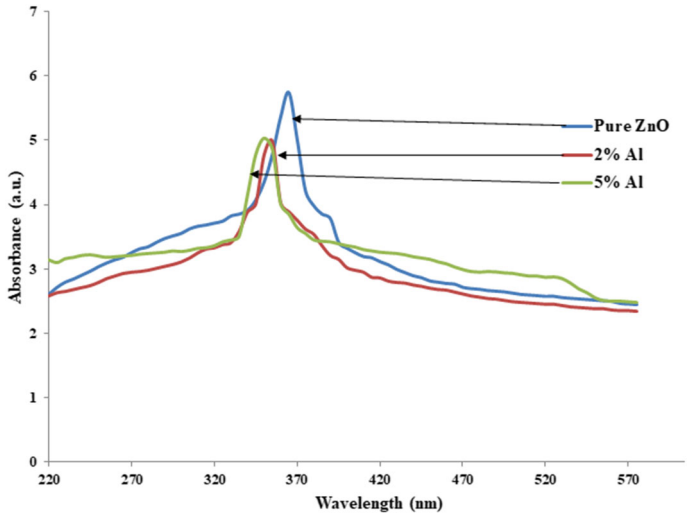

Fig. 6 UV absorption analysis of pure ZnO and Al-doped ZnO nanostructures

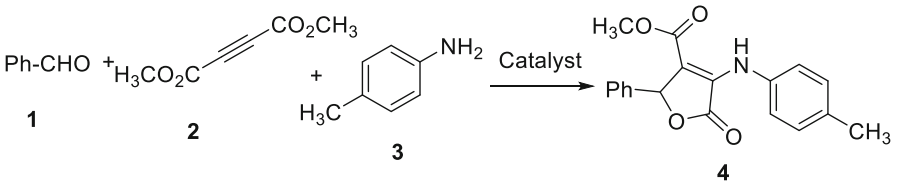

Scheme 2 Preparation of methyl 4-(*p*-tolylamino)-2,5-dihydro-5-oxo-2-phenylfuran-3-carboxylate

Table 2 Catalyst screening

Entry	Catalyst (0.6 mmol)	Yield (%)[a]
1	SnO_2	30
2	Al_2O_3	–
3	SiO_2	–
4	Fe_2O_3	–
5	MgO	65
6	CaO	–
7	ZnO	80
8	Al-doped ZnO (2% Al)	85
9	Al-doped ZnO (5% Al)	84

[a]Isolated yields; reaction condition: solvent: EtOH, reflux, time: 8 h

Table 3 Optimization of the reaction condition in the synthesis of methyl 2,5-dihydro-5-oxo-2-phenyl-4-(phenylamino)furan-3-carboxylate

Entry	Catalyst (mmol)	*T* (°C)	Solvent (5 mL)	Time (h)	Yield (%)[a]
1	0.6	Reflux	*n*-Hexane	10	–
2	0.6	Reflux	CH_2Cl_2	10	–
3	0.6	Reflux	Et_2O	10	–
4	0.6	Reflux	EtOAc	10	15
5	0.6	Reflux	EtOH	8	85
6	0.6	Reflux	MeOH	8	79
7	0.6	r.t.	Solvent-free	10	–
8	–	r.t.	EtOH	10	–
9	0.3	Reflux	EtOH	8	87
10	0.8	Reflux	EtOH	8	86
11	1	Reflux	EtOH	8	84

r.t. Room temperature

[a]Isolated yields

aromatic aldehydes strongly dependent on the electronic nature of the aldehyde. Electron-rich aldehydes are more efficient substrates than those bearing electron-withdrawing substituents. The reaction of *p*-methylbenzaldehyde was completed in

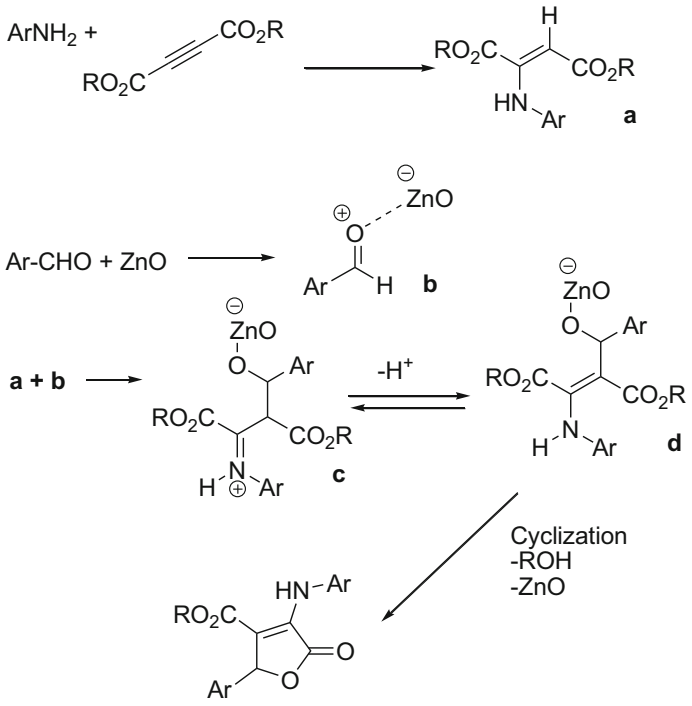

Scheme 3 Proposed mechanism for the formation of 3,4,5-substituted furan-2(5*H*)-ones

shorter reaction time and is higher-yielding than 4-chlorobenzaldehyde (Table 4, entries **1a**–**7a**).

On the other hand, during the reaction course, the nucleophilic Michael addition of the aromatic amines to the dialkyl acetylenedicarboxylate generates the aminobutendioate as an electron-rich enaminone and an active nucleophile. Aromatic amines that are substituted by EDGs such as 4-methyl or 3,4-dimethyl (Table 4) are more reactive intermediates than those of EWGs such as chlorine (Table 4, entries **8a**–**9a**).

The other factor that influences the reaction rate is steric hindrance. 2-Chlorobenzaldehyde afforded the product in lower yield in longer reaction time, probably because of steric hindrance (Table 4, entries **15a**, **16a**, **17a**).

Noticeably, we found that the above reactions could lead to the desired products under ultrasonic irradiation condition in high yields and shorter reaction times; the results are summarized in Table 4.

The ^{1}H-NMR spectrum (in DMSO-d_6) of compound **22a** as a model showed a singlet related to the $\mathbf{H_a}$ (furanone sp^3 proton) at δ = 6.48 ppm. A singlet appearing at δ = 10.14 was assigned to an N–H proton. The aromatic protons from the *ortho* position of the amine moiety appear as a doublet at 6.69 ppm and a singlet at around 6.80–6.87 which is overlapped with the only *meta* proton of the amine ring. The

Table 4 Synthesis of 3,4,5-substituted furan-2(5*H*)-one derivatives (Scheme 1)

Product	Aldehyde	Amine	R	A Time (h)/yield (%)[a]	B Time (h)/yield (%)[a]
1a	Benzaldehyde	4-Methylaniline	**Me**	8/87	4/90
2a	Benzaldehyde	4-Methylaniline	**Et**	8/89	4/85
3a	4-Methylbenzaldehyde	4-Methylaniline	**Me**	7/93	4/95
4a	4-Methylbenzaldehyde	4-Methylaniline	**Et**	7/88	4/86
5a	4-Chlorobenzaldehyde	4-Methylaniline	**Me**	8/89	4/93
6a	4-*tert*-Butylbenzaldehyde	4-Methylaniline	**Me**	7/93	4/90
7a	4-*tert*-Butylbenzaldehyde	4-Methylaniline	**Et**	7/87	4/86
8a	4-Methylbenzaldehyde	4-Chloroaniline	**Me**	9/86	5/87
9a	Benzaldehyde	4-Chloroaniline	**Me**	10/85	5/89
10a	4-Methylbenzaldehyde	4-Methoxyaniline	**Me**	6/96	3/91
11a	Benzaldehyde	Aniline	**Me**	8/87	4/84
12a	Benzaldehyde	Aniline	**Et**	10/85	5/90
13a	4-Methylbenzaldehyde	Aniline	**Me**	8/86	4/85
14a	4-Methylbenzaldehyde	Aniline	**Et**	9/87	5/80
15a	4-Chlorobenzaldehyde	Aniline	**Me**	11/86	7/92
16a	2-Chlorobenzaldehyde	Aniline	**Me**	12/81	8/83
17a	2,4-Dichlorobenzaldehyde	Aniline	**Me**	15/80	8/86
18a	Benzofuran-2-carbaldehyde	Aniline	**Me**	10/93	6/92
19a	Benzofuran-2-carbaldehyde	Aniline	**Et**	12/90	7/91
20a	Benzofuran-2-carbaldehyde	4-Methylaniline	**Me**	10/94	6/90
21a	Benzofuran-2-carbaldehyde	4-Methylaniline	**Et**	11/86	7/96
22a	Benzofuran-2-carbaldehyde	3,4-Dimethylaniline	**Me**	10/88	6/94
23a	Benzofuran-2-carbaldehyde	3,4-Dimethylaniline	**Et**	11/89	7/80
24a	Benzaldehyde	3,4-Dimethylaniline	**Me**	8/93	4/86
25a	Benzaldehyde	3,4-Dimethylaniline	**Et**	9/86	4/89
26a	4-Methylbenzaldehyde	3,4-Dimethylaniline	**Me**	8/97	4/93
27a	4-Methylbenzaldehyde	3,4-Dimethylaniline	**Et**	8/92	4/90
28a	4-Chlorobenzaldehyde	3,4-Dimethylaniline	**Me**	10/86	6/87
29a	3-Chlorobenzaldehyde	3,4-Dimethylaniline	**Me**	10/84	6/89
30a	2-Chlorobenzaldehyde	3,4-Dimethylaniline	**Me**	12/96	7/91
31a	4-*tert*-Butylbenzaldehyde	3,4-Dimethylaniline	**Me**	8/89	4/85
32a	4-Methoxybenzaldehyde	3,4-Dimethylaniline	**Me**	8/89	4/87
33a	3-Methoxybenzaldehyde	3,4-Dimethylaniline	**Me**	8/90	4/87
34a	2-Methylbenzaldehyde	3,4-Dimethylaniline	**Me**	10/84	6/89

[a]Isolated yields. A: EtOH, reflux; B: EtOH, 70 °C, ultrasonic irradiation. Products **1a**–**17a** are reported previously [24–32], and products **18a**–**34a** are new and were characterized by their NMR and CHN analysis

Scheme 4 Structure of methyl 4-(3,4-dimethylphenylamino)-2-(benzofuran-2-yl)-2,5-dihydro-5-oxofuran-3-carboxylate (compound **22a**)

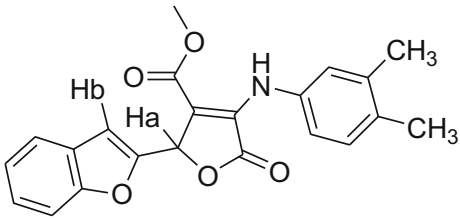

proton assigned as $\mathbf{H_b}$ (Scheme 4) appears at δ = 7.41 as a singlet. Two multiplets appearing at around 7.25–7.31 and 7.51–7.56 ppm are related to aromatic protons of the benzofuran moiety. Finally, three singlets appearing at 2.21, 2.25, and 3.75 integrated for *para* methyl, *meta* methyl, and methoxy protons, respectively.

The ^{13}C-NMR spectrum of compound **22a** showed 22 distinct resonances. Some of them are assigned as 19.8 (CH_3), 20.7 (CH_3), 52.3 (OCH_3), 73.2 (C-sp^3 benzylic furanone ring), 162.1 (–$COOCH_3$), and 165.1 (COO furanone ring) ppm.

Significantly, after completion of the reaction, the catalyst could be successfully recovered from the crude reaction mixture and reused for further catalytic cycles. The results of catalyst recovery showed that the catalyst could be recycled five times without apparent decrease in the catalytic efficiency (Fig. 7). Moreover, our investigation revealed that the catalyst is stable in the reaction conditions and its structure does not change after recovery. The XRD patterns of fresh and reused catalyst are shown in Fig. 8 and confirm the stability of the catalyst.

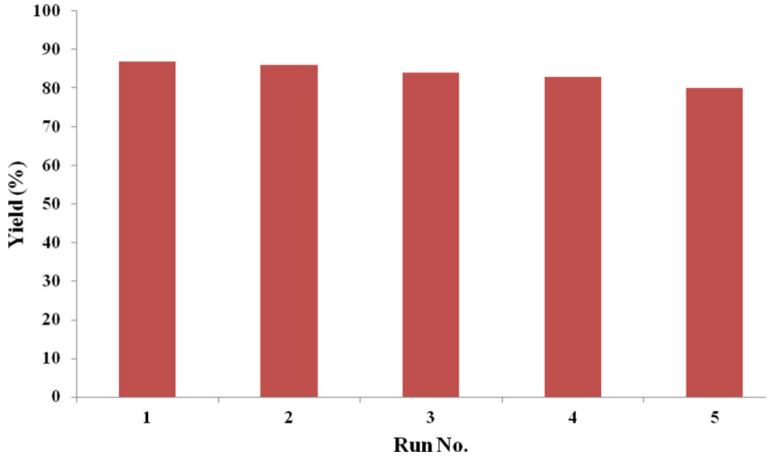

Fig. 7 Reusability of Al-doped ZnO nanostructure (2% Al) as a catalyst

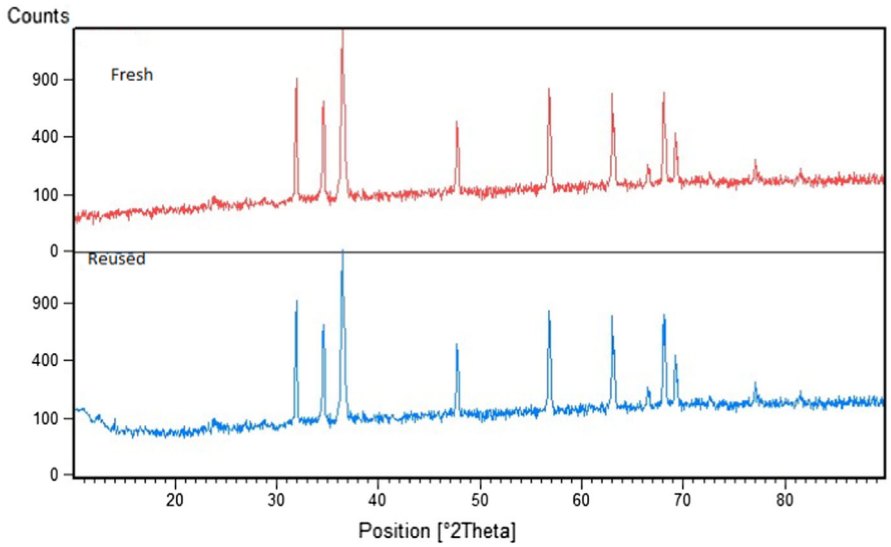

Fig. 8 The XRD patterns of fresh and reused Al-doped ZnO nanostructure (2% Al) as a catalyst

Conclusion

In summary, nanostructured Al-doped ZnO was prepared via a simple precipitation method and was applied as a mild and efficient green catalyst for the syntheses of 3,4,5-substituted furan-2(5*H*)-one derivatives. Various substituted amines and aldehydes were used in the reaction. All products were obtained in good to excellent yields. From the standpoint of the reaction conditions, it can be said that the advantages of this method are mild conditions and high yields.

Acknowledgements We are thankful to the Najafabad Branch of the Islamic Azad University Research Council for partial support of this research.

References

1. B. Clark, R.J. Capon, E. Lacey, S. Tennant, J.H. Gill, B. Bulheller, G. Bringmann, J. Nat. Prod. **68**, 1226 (2005)
2. M.M. Baag, N.P. Argade, Synthesis **2008**, 26 (2008)
3. S.-C. Lee, G.D. Brown, J. Nat. Prod. **61**, 29 (1998)
4. M. Seitz, O. Reiser, Curr. Opin. Chem. Biol. **9**, 285 (2005)
5. T.M. Ugurchieva, V.V. Veselovsky, Russ. Chem. Rev. **78**, 337 (2009)
6. Y.S. Rao, Chem. Rev. **76**, 625 (1976)
7. X. Jusseau, L. Chabaud, C. Guillou, Tetrahedron **70**, 2595 (2014)
8. R. Rossi, F. Bellina, M. Biagetti, L. Mannina, Tetrahedron Lett. **39**, 7799 (1998)
9. L.M. Levy, G.M. Cabrera, J.E. Wright, A.M. Seldes, Phytochemistry **62**, 239 (2003)
10. S.M. Hein, J.B. Gloer, B. Koster, D. Malloch, J. Nat. Prod. **64**, 809 (2001)
11. M. Pour, M. Spulak, V. Balsanek, J. Kunes, P. Kubanova, V. Butcha, Bioorg. Med. Chem. **11**, 2843 (2003)
12. S. Padakanti, M. Pal, K.R. Yeleswarapu, Tetrahedron **59**, 7915 (2003)
13. T.R. Hoye, L. Tan, Tetrahedron Lett. **36**, 1981 (1995)

14. S. Takahashi, A. Kubota, T. Nakata, Tetrahedron Lett. **43**, 8661 (2002)
15. S. Hanessian, R.Y. Park, R.Y. Yang, Synlett **1997**, 351 (1997)
16. A. Choudhury, F. Jin, D. Wang, Z. Wang, G. Xu, D. Nguyen, J. Castoro, M.E. Pierce, P.N. Confalone, Tetrahedron Lett. **44**, 247 (2003)
17. B. Beck, M. Magnin-Lachaux, E. Herdtweck, A. Dömling, Org. Lett. **3**, 2875 (2001)
18. E. Genin, P.Y. Toullec, S. Antoniotti, C. Brancour, J.-P. Genêt, V. Michelet, J. Am. Chem. Soc. **128**, 3112 (2006)
19. Q. Zhang, M. Cheng, X. Hu, B.-G. Li, J.-X. Ji, J. Am. Chem. Soc. **132**, 7256 (2010)
20. S. Ma, Z. Shi, J. Org. Chem. **63**, 6387 (1998)
21. Y. Wu, W. Yao, L. Pan, Y. Zhang, C. Ma, Org. Lett. **12**, 640 (2010)
22. Y.-Q. Zhu, T.-F. Han, J.-L. He, M. Li, J.-X. Li, K. Zhu, J. Org. Chem. **82**, 8598 (2017)
23. B.R. Park, K.H. Kim, J.W. Lim, J.N. Kim, Tetrahedron Lett. **53**, 36 (2012)
24. S.N. Murthy, B. Madhav, A. Vijay Kumar, K. Rama Rao, Y.V.D. Nageswar, Tetrahedron **65**, 5251 (2009)
25. L. Nagarapu, U.N. Kumar, P. Upendra, R. Bantu, Synth. Commun. **42**, 2139 (2012)
26. S.U. Tekale, S.S. Kauthale, V.P. Pagore, V.B. Jadhav, R.P. Pawar, J. Iran. Chem. Soc. **10**, 1271 (2013)
27. M.R. Mohammad Shafiee, M. Kargar Biointerface, Res. Appl. Chem. **7**, 2170 (2017)
28. M.R. Mohammad Shafiee, S.S. Mansoor, M. Ghashang, A. Fazlinia, Compt. Rend. Chim. **17**, 131 (2014)
29. R. Doostmohammadi, M.T. Maghsoodlou, N. Hazeri, S.M. Habibi-Khorassani, Chin. Chem. Lett. **24**, 901 (2013)
30. R. Doostmohammadi, N. Hazeri, Lett. Org. Chem. **10**, 199 (2013)
31. J. Safaei-Ghomi, E. Heidari-Baghbahadorani, H. Shahbazi-Alavi, Monatsh. Chem. **146**, 181 (2015)
32. F. Bahramian, A. Fazlinia, S.S. Mansoor, M. Ghashang, F. Azimi, M.N. Biregan, Res. Chem. Intermed. **42**, 6501 (2016)
33. M. Ghashang, Curr. Org. Synth. **9**, 727 (2012)
34. M. Ghashang, S.S. Mansoor, K. Aswin, Chin. J. Catal. **35**, 127 (2014)
35. H. Taghrir, M. Ghashang, M. Najafi Biregan, Chin. Chem. Lett. **27**, 119 (2016)
36. M. Ghashang, Res. Chem. Intermed. **42**, 4191 (2016)
37. M. Ghashang, M. Kargar, M.R.M. Shafiee, S.S. Mansoor, A. Fazlinia, H. Esfandiari, Recent Pat. Nanotechnol. **9**, 204 (2015)
38. M. Ghashang, S.S. Mansoor, M.R. Mohammad Shafiee, M. Kargar, M. Najafi Biregan, F. Azimi, H. Taghrir, J. Sulfur Chem. **37**, 377 (2016)
39. A. Baziar, M. Ghashang, React. Kinet. Mech. Catal. **118**, 463 (2016)
40. M. Ghashang, S.S. Mansoor, L. Shams Solaree, A. Sharifian-esfahani, Iran. J. Catal. **6**, 237 (2016)
41. M.R. Mohammad Shafiee, M. Kargar, M.S. Hashemi, M. Ghashang, Curr. Nanosci. **12**, 645 (2016)
42. M. Ghashang, Biointerface Res. Appl. Chem. **6**, 1338 (2016)
43. N. Sheikhan-Shamsabadi, M. Ghashang, Main Group Met. Chem. **40**, 19 (2016)
44. M.R. Mohammad Shafiee, A. Sattari, M. Kargar, M. Ghashang, Steel Compos. Struct. **24**, 15 (2016)
45. M.M. Hassan, W. Khan, A. Azam, A.H. Naqvi, J. Lumin. **145**, 160 (2014)
46. M.A.M. Khan, S. Kumar, M.N. Khan, M. Ahamed, A.S. Al Dwayyan, J. Lumin. **155**, 275 (2014)